

The distribution and physical properties of high-redshift [OIII] emitters in a cosmological hydrodynamics simulation

Kana Moriwaki

Department of Physics, The University of Tokyo, 7-3-1 Hongo, Bunkyo, Tokyo 113-0033, Japan
email: kana.moriwaki@utap.phys.s.u-tokyo.ac.jp

Abstract. Atacama Large Millimeter/submillimeter Array (ALMA) has enabled us to detect [OIII] 88 μm line even at $z > 9$. To study the properties of high-redshift [OIII] emitters, we calculate [OIII] luminosities of galaxies in a cosmological simulation by applying a physical model of HII region and using the photoionization code CLOUDY. We find that the [OIII] 88 μm luminosity, $L_{\text{OIII},88}$, scales with SFR with slightly larger $L_{\text{OIII},88}$ than a local relation. Some [OIII] emitters have extended disk-like structure. We propose to use the ratio between [OIII] 88 μm line and [OIII] 5007 Å line, which can be detected with James Webb Space Telescope (JWST), to estimate the gas density and the metallicity in HII region of high-redshift [OIII] emitters.

Keywords. galaxies: formation, galaxies: high-redshift, galaxies: ISM

1. Introduction

It is important to study the high-redshift galaxies at the epoch of reionization. After Hubble Space Telescope has detected many high-redshift galaxy candidates using dropout techniques, the spectroscopic identifications have primarily been done with hydrogen Ly α line. However, Ly α emission becomes increasingly weak at $z > 7$ due to the attenuation by the neutral hydrogen in the intergalactic medium before the completion of the reionization (e.g. [Konno et al. 2014](#)).

Thanks to the ALMA, we can now use far-infrared (FIR) lines instead of Ly α . While [CII] 158 μm line is the brightest line in local star-forming galaxies, [OIII] 88 μm line is brighter than [CII] 158 μm in local dwarf galaxies ([Lebouteiller et al. 2012](#); Cormier et al. 2015). Motivated by this, [Inoue et al. \(2014\)](#) suggested to use [OIII] 88 μm line for the spectroscopic redshift identification of distant galaxies. Recently, [OIII] 88 μm lines have been detected in several galaxies at $z > 7$ ([Inoue et al. 2016](#); [Carniani et al. 2017](#); [Laporte et al. 2017](#); [Hashimoto et al. 2018a](#); [Hashimoto et al. 2018b](#); [Tamura et al. 2018](#)).

Line emission can also be used to study the properties of galaxies. For example, rotation signature can be seen with line-of-sight velocity gradient (e.g. [Smit et al. 2018](#)). Also, emission line diagnostics using either optical or FIR lines to estimate the property of the interstellar medium are well studied (e.g. [Nagao et al. 2011](#)). Since ALMA and JWST provide us access to both FIR and optical lines, diagnostics using lines in both wavelength should also be considered.

2. Methods

To study the typical properties of high-redshift [OIII] emitters, we use a cosmological hydrodynamics simulation of [Shimizu et al. \(2016\)](#) using GADGET-3. This simulation has

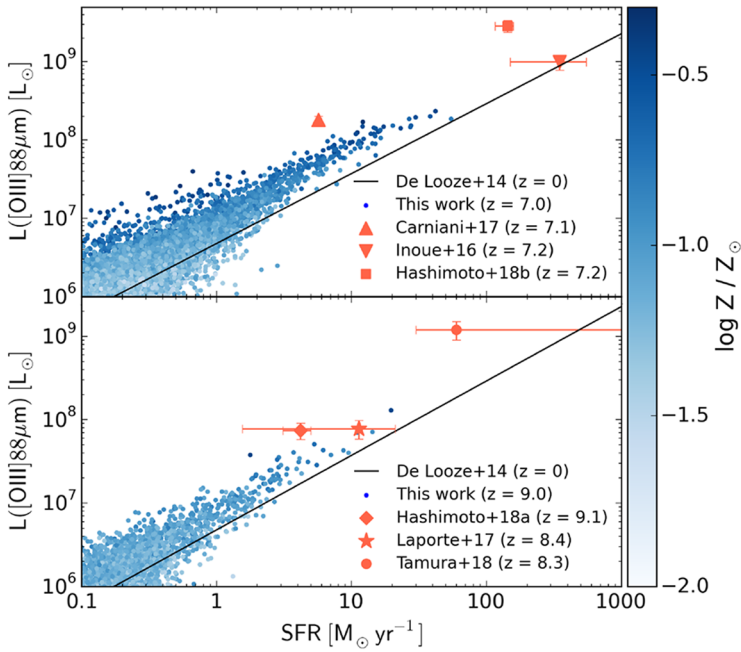


Figure 1. [OIII]-SFR relation of simulation galaxies (Moriwaki *et al.* 2018) and observed galaxies (Inoue *et al.* 2016; Carniani *et al.* 2017; Laporte *et al.* 2017; Hashimoto *et al.* 2018a; Hashimoto *et al.* 2018b; Tamura *et al.* 2018) at $z \sim 7$ (upper) and ~ 9 (bottom). The solid line is the local relation derived by De Looze *et al.* (2014).

a boxsize of a comoving $50h^{-1}$ Mpc cube. The number of particles is 2×1280^3 for dark matter ($m_{\text{DM}} = 4.44 \times 10^6 h^{-1} M_\odot$) and gas ($m_{\text{gas}} = 8.11 \times 10^5 h^{-1} M_\odot$). See Shimizu *et al.* (2016) for more details.

The detail calculation method of line luminosities is found in Moriwaki *et al.* (2018). Briefly, we use CLOUDY (Ferland *et al.* 2013) to generate a table of line luminosities with various sets of gas metallicity, ionization parameter, and gas density as in Inoue (2011) and Inoue *et al.* (2014). Then we calculate the line luminosity of each star particle by assuming that a spherical HII region forms around it.

3. Results

Fig. 1 shows the [OIII] $88\mu m$ luminosity, $L_{\text{OIII},88}$, and SFR of simulation galaxies at $z = 7$ and 9. The solid line is the $L_{\text{OIII},88}$ -SFR relation in local galaxies (De Looze *et al.* 2014). We find that $L_{\text{OIII},88}$ scales with SFR and the [OIII] emitters with $L_{\text{OIII},88} > 10^8 L_\odot$ has $\text{SFR} > 10 M_\odot \text{ yr}^{-1}$. They reside in massive haloes with masses $> 10^{11} M_\odot$ and the typical metallicity is $\sim 0.1 Z_\odot$. These indicate that well-established galaxies are selectively observed at this early universe. Our model predicts slightly larger $L_{\text{OIII},88}$ than those expected from the local relation due to the high ionization parameters and the metallicities.

Brightest [OIII] emitters have as large size as 1 kpc, which corresponds to $\sim 0.2''$ at $z \sim 7$. These extended galaxies have a disk-like structure and rotation velocity $\sim 50 \text{ km s}^{-1}$. In some [OIII] emitters, there is displacement between [OIII] emission and entire stellar distribution. Since [OIII] emission traces the young stellar population, this indicates the inside-out star formation history.

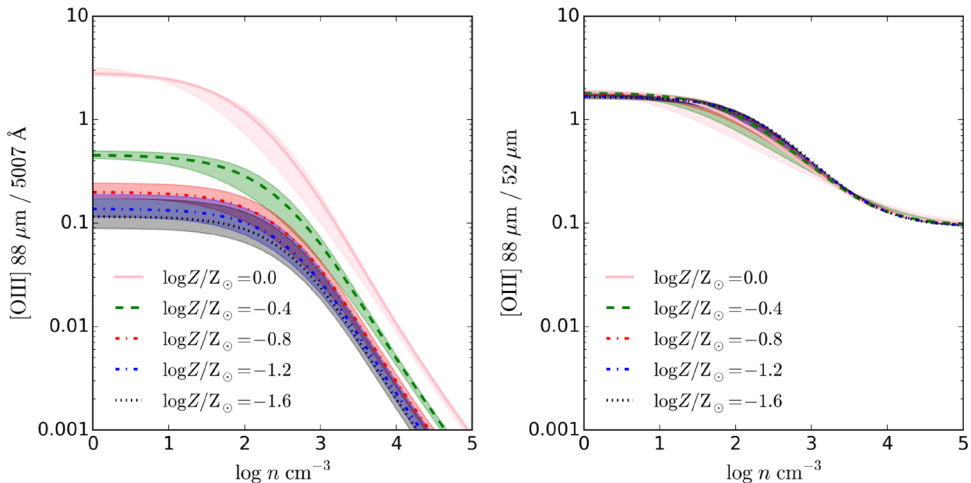


Figure 2. The line ratios of $[\text{OIII}] 88 \mu\text{m} / 5007 \text{\AA}$ (left) and $[\text{OIII}] 88 \mu\text{m} / 52 \mu\text{m}$ (right) calculated with CLOUDY. Each line shows the line ratios with ionization parameter $U = 10^{-2}$ and fixed metallicities. The filled region of each color corresponds to ionization parameter range from $U = 10^{-3}$ to 10^{-1} . The input stellar continuum is calculated by assuming constant star formation duration of 10 Myr.

4. Discussion

The $[\text{OIII}] 5007 \text{\AA}$ line is roughly an order of magnitude larger than the $[\text{OIII}] 88 \mu\text{m}$ line, whereas the typical detection limits of JWST is only ~ 3 times worse than that of ALMA. So, when ALMA already discovered the $[\text{OIII}] 88 \mu\text{m}$ emission from a galaxy, then JWST can always detect $[\text{OIII}] 5007 \text{\AA}$ emission from that galaxy too. With the high angular resolution of ALMA and JWST, we can study the structure and the kinematics of bright $[\text{OIII}]$ emitters.

Since $[\text{OIII}] 88 \mu\text{m}$ and $[\text{OIII}] 5007 \text{\AA}$ lines have different critical densities and excitation temperatures, the ratio between them depends on the temperature and the density of the HII region. The temperature also depends on the gas metallicity because the metallicity controls the cooling efficiency. We show the $[\text{OIII}] 88 \mu\text{m} / 5007 \text{\AA}$ line ratio calculated with CLOUDY in the left panel of Fig. 2. The ratio decreases near the critical density of $[\text{OIII}] 88 \mu\text{m}$, $\sim 500 \text{ cm}^{-3}$. At lower metallicity or higher ionization parameter, $[\text{OIII}] 5007 \text{\AA}$ is stronger due to high temperature and the ratio decreases. Although there is a degeneracy between parameters, properties of HII region can be extracted from this line ratio to some extent; if the ratio is greater than 0.3, then it indicates that the metallicity is larger than $\sim 0.2 Z_\odot$, or if the ratio is much lower than 0.1, then the gas density is much higher than 100 cm^{-3} . If galaxies have as high density as 1000 cm^{-3} , $[\text{OIII}] 52 \mu\text{m}$ line is brighter than $[\text{OIII}] 88 \mu\text{m}$ and can be detected with ALMA. As shown in the right panel of Fig. 2, $[\text{OIII}] 88 \mu\text{m} / 52 \mu\text{m}$ ratio provide us the gas density without any degeneracy. If the gas density is fixed, the temperature or the metallicity can be more constrained from $[\text{OIII}] 88 \mu\text{m} / 5007 \text{\AA}$ ratio. Though we need to consider dust attenuation especially for $[\text{OIII}] 5007 \text{\AA}$ line, this diagnostics still works well for galaxies with little dust extinction. For instance, when the dust extinction A_V is 0.3, the difference between observed and intrinsic line ratios is only 0.1 dex and it is negligible.

It is possible to detect the large-scale structure by performing $[\text{OIII}]$ line survey. Here, we consider a survey of $[\text{OIII}] 5007 \text{\AA}$ line emitters with JWST NIRCam. There are two possible ways: using grism module with F444W filter and using narrow-band F466N filter. We calculate the average number of $[\text{OIII}]$ emitters within a field of view of $2 \times 2.2' \times 2.2'$

that can be detected with $S/N > 5$ by assuming 10^4 s integration. We find that we can detect ~ 2 [OIII] emitters at $6.8 < z < 9.0$ with grism module and ~ 0.5 at $z = 8.3$ with narrow band. We can remove the foreground H α contaminants at $z \sim 6$ by J-dropout technique. For grism module, detecting doublet [OIII] 4959, 5007 Å also help us to distinguish these two lines.

References

- Carniani, S., Maiolino, R., Pallottini, A., Vallini, L., Pentericci, L., et al. 2017, *A&A*, 605, A42
 De Looze, I., Cormier, D., Lebouteiller, V., Madden, S., Baes, M., et al. 2014, *A&A*, 568, A62
 Ferland, G. J., Porter, R. L., van Hoof, P. A. M., Williams, R. J. R., Abel, N. P., et al. 2013,
Rev. Mexicana AyA, 49, 137
 Hashimoto, T., Laporte, N., Mawatari, K., Ellis, R. S., Inoue, A. K., et al. 2018a, *Nature*,
 557, 392
 Hashimoto, T., Inoue, A. K., Mawatari, K., Tamura, Y., Matsuo, H., et al. 2018b,
[ArXiv:1806.00486](https://arxiv.org/abs/1806.00486)
 Inoue, A. K. 2011, *MNRAS*, 415, 2920
 Inoue, A. K., Shimizu, I., Tamura, Y., Matsuo, H., Okamoto, T., & Yoshida, N. 2014, *ApJ*,
 780, L18
 Inoue, A. K., Tamura, Y., Matsuo, H., Mawatari, K., Shimizu, I., et al. 2016, *Science*, 352, 1559
 Konno, A., Ouchi, M., Ono, Y., Shimasaku, K., Shibuya, T., et al. 2014, *ApJ*, 797, 16
 Laporte, N., Ellis, R. S., Bauer, F. E., Quénard, D., Roberts-Borsani, G. W., et al. 2017, *ApJ*,
 837, L21
 Lebouteiller, V., Cormier, D., Madden, S. C., Galliano, F., Indebetouw, R., et al. 2012, *A&A*,
 548, A91
 Moriwaki, K., Yoshida, N., Shimizu, I., Harikane, Y., Matsuda, Y., et al. 2018, *MNRAS*, 481, L84
 Nagao, T., Maiolino, R., Marconi, A., & Matsuhabara, H. 2011 *A&A*, 526, A149
 Shimizu, I., Inoue, A. K., Okamoto, T., & Yoshida, N. 2016, *MNRAS*, 461, 3563
 Smit, R., Bouwens, R. J., Carniani, S., Oesch, P. A., Labb  , I., et al. 2018, *Nature*, 553, 178
 Tamura, Y., Mawatari, K., Hashimoto, T., Inoue, A. K., Zackrisson, E., et al. 2018,
[ArXiv:1806.04132](https://arxiv.org/abs/1806.04132)